Chemical Engineering Journal 165 (2010) 537–544

Contents lists available at ScienceDirect

Chemical Engineering Journal

journal homepage: www.elsevier.com/locate/cej

Artemisia vulgaris-derived mesoporous honeycomb-shaped activated carbon for ibuprofen adsorption

Shashi Prabha Dubey[a,*], Amarendra Dhar Dwivedi[b], Mika Sillanpää[a,c], Krishna Gopal[b]

[a] *Laboratory of Applied Environmental Chemistry, Department of Environmental Sciences, University of Eastern Finland, FI-50100 Mikkeli, Finland*
[b] *Aquatic Toxicology Division, Indian Institute of Toxicology Research (CSIR), M.G. Marg, P.O. Box 80, Lucknow 226001, U.P., India*
[c] *Faculty of Technology, Lappeenranta University of Technology, Patteristonkatu 1, FI-50100 Mikkeli, Finland*

ARTICLE INFO

Article history:
Received 10 June 2010
Received in revised form
27 September 2010
Accepted 29 September 2010

Keywords:
Ibuprofen
Langmuir–Freundlich
Mesoporous carbon
Mugwort
ζ Potential

ABSTRACT

The purpose of the present work was to synthesize a novel mesoporous activated carbon from an invasive weed to investigate its potential application for removal of the emerging organic contaminants in waters. The worldwide highly consumable non-steroidal anti-inflammatory drug (NSAID); ibuprofen (Ibu), was chosen for the study due to its toxicity and global occurrence in waters. Keeping this in mind, *Artemisia vulgaris* (common name: Mugwort) leaves were processed by physical and chemical activation to obtain the mesoporous honeycomb-structured activated carbon (MAC) to mitigate Ibu. To understand the activity of the activated carbon towards contaminant, adsorption batch mode process was investigated for the solid–liquid phase characteristics of Ibu–water system. Both kinetic and equilibrium models were evaluated over a wide range of conditions to determine the rate laws and maximum Ibu uptake capacity. A decisive reliance of adsorption capacity on pH was observed in pH range from 2 to 9. The high surface area (358.20 m^2/g), mesoporosity (2.46 nm) and surface functionality of MAC played significant role in Ibu uptake. Plausible mechanistic findings for adsorptive mitigation were substantiated by spectroscopic techniques viz. SEM, FTIR, EDX and ζ potentiometry.

1. Introduction

The proliferation in variety of different chemicals released in the environment has gone beyond the point of no return due to rapid industrialization. Emerging contaminants of concern, including inorganic and organic chemicals, are released into the aquatic systems, so, is matter of global anxiety before environmentalists [1–3]. In recent years, due to their widespread occurrence in aquatic environments, pharmaceutical compounds have been recognized as a major group of emerging pollutants. Endocrine disrupting chemicals (EDCs) are prevalent in food chains as they are vast group of chemical entities of different origin and functionalities. EDCs comprise one of the major classes of non-steroidal anti-inflammatory drugs (NSAIDs).

Ibuprofen is one of the most highly utilized NSAIDs worldwide [4] and therefore it has been one of the most commonly detected pharmaceuticals in the environment, with concentrations up to micrograms per liter [5]. EDCs are active environmental entities that may influence the metabolism, transport and synthesis of natural hormones in the body even at very low concentrations [6]. A number of studies have been performed in countries such as Germany, Spain, Switzerland, France, Italy, Sweden, Canada and Denmark and have found concentrations of ibuprofen in wastewater effluents varying from 60 to 3400 ng/L [7–11].

Membrane filtration (nanofiltration and reverse osmosis) [12], UV-degradation [13], ultrasonic degradation [14] and electrochemical degradation [15] have been reported for NSAID removal from surface or drinking water. The drawbacks to these methods, such as toxic sludge generation, incomplete removal, very high capital and running costs, high-tech operations and skilled personnel requirements, make them unsuccessful methods, and they cannot currently be considered viable options. To avert NSAID outflows to the environment, there is an urgent need to investigate robust treatment methods for mitigation procedures which do not require high cost equipment or highly specialized human resources, and which are environmental friendly and address local resources and constraints. In this connection, many researchers have recently shown an interest in Ibu adsorption using submerged surface flow-constructed wetlands, coconut-shell activated carbon, zeolites, microcosm constructed wetlands, commercial carbon from coal, mesoporous silica, SBA-15 and activated carbon [16–21]. The major advantages of adsorption processes are high efficiency, easy operations and simple design.

Herein, we reported our efforts to improve the efficacy of an invasive weed towards Ibu removal. *Artemisia vulgaris* (common

* Corresponding author.
E-mail addresses: shashiprabhadubey@gmail.com, shashi.dubey@uef.fi (S.P. Dubey).

1385-8947/$ – see front matter © 2010 Elsevier B.V. All rights reserved.
doi:10.1016/j.cej.2010.09.068

Nomenclature

AAS	atomic absorption spectrophotometer
GC-FID	gas chromatography-flame ionization detector
q_e	amount of adsorbate on adsorbent at equilibrium (mg/g)
q_t	capacity of adsorbent at time t
C_0	initial concentrations (mg/L) of adsorbate
C_e	equilibrium concentrations (mg/L) of adsorbate
M_{MAC}	amount of MAC added in solution (g/L)
Q_m	maximum adsorption capacity (mg/g)
k_l	Langmuir constant related to the free energy of adsorption (L/mg)
k_f	Freundlich constant representing adsorption capacity
n_f	Freundlich constant representing intensity of adsorption
k_{lf}	coefficient of Langmuir–Freundlich equation
n	coefficient of Langmuir–Freundlich equation
k_1	pseudo first order (min^{-1})
k_2	pseudo second order rate constant (g/mg min)
α	the initial adsorption rate (mg/g h)
β	the rate of chemisorptions (g/mg) at zero coverage
k_{ipd}	the intra particle diffusion rate constant (mg/g h)
C	intraparticle diffusion constant
R	universal gas constant (8.314 J/mol K)
T	absolute temperature (K)
K	thermodynamic equilibrium constant
ΔG°	free energy change of the reaction (J/mol)
ΔH°	enthalpy change of the adsorption (J/mol)
ΔS°	entropy change of the adsorption (J/mol K)
S.D.	standard deviation
r^2	correlation coefficient
χ^2	reduced chi square

name: mugwort) is a kind of invasive weed that has adverse economic, environmental and ecological effects on the habitats it invades. This plant is known as *nagadamni* in Sanskrit [22]. A weed is a native or nonnative plant that grows and reproduces aggressively and which is considered by the user to a nuisance, and is unwanted in human-made settings such as gardens, lawns or agricultural areas, as well as in parks, woods and other natural areas. Mugwort contains thujone, which is toxic in large amounts or with prolonged intake. Mugwort pollen is one of the main sources of hay fever and allergic asthma in Northern Europe, North America and in some parts of Asia [23].

In continuation of our interest in the search of potent adsorbents from natural materials, we have explored the potential of mugwort for use in the mitigation of water-borne poisons in water reclamation processes with our findings in this article.

2. Materials and methods

Ibuprofen, methanol and *N*,*O*-bis(trimethylsilyl)trifluoroacetamide (BSTFA) were purchased from Sigma–Aldrich. Ultrapure water was used to prepare the standard solutions. 250 mg/L of Ibu solution was prepared in methanol and diluted to 10 mg/L with addition of ultra pure water. The final percentage of methanol did not exceed 0.1% (v/v), so it would not have had any influence on experimental procedures.

2.1. Production of mugwort-derived activated carbon (MAC)

The leaves of Mugwort used in the present investigations were procured locally during the months of June and July from Mikelli, Finland, which was growing in plenty along the garden side. It was thoroughly washed with distilled water to remove any dirt, dried, crushed and sieved to a particle size of 2–3 mm. 20 g of this material was treated with 30 mL of 60% (v/v) sulphuric acid solution for 8–12 h. The sample was left overnight and washed with ultrapure water until the pH was 6–7, and dried at 120 °C for 6 h. The dried carbonized sample was heated in a stream of nitrogen at a rate of 3 °C min^{-1} up to 450 °C and held there for 30 min. After reaching the activation temperature, the material was cooled in nitrogen atmosphere. After cooling, the material was washed with ultrapure water until the pH was 6.8 ± 0.2, and then dried at 120 °C and stored in a dessicator for sorption experiments.

2.2. Characterizations of MAC

2.2.1. Physical characterizations

The prepared MAC was characterized by N_2 adsorption/desorption. This was carried out on a Quantachrome Autosorb Automated Gas Sorption System, from which the BET surface area, the pore volume and the pore size were obtained. The sample was de-gassed at 350 °C for 20 h prior to adsorption. The pore volume of the mesoporous activated carbon was calculated from the adsorbed nitrogen after complete pore condensation ($P/P_0 = 0.995$) using the ratio of the densities of liquid and gaseous nitrogen.

The ash content of the activated carbon was determined by weighing the residue left after combustion of the sample in air at 650 °C (3 h) according to the standard method previously described [24]. Initially the crucible was ignited for 1 h and cooled to room temperature. Then 1.5 g of the adsorbent was placed in the crucible and dried to a constant weight at 150 ± 5 °C for 3 h. Then the crucible was placed in a furnace at 650 °C for 3 h. After cooling the sample in a desiccator, the constant weight was measured. Loss on ignition was calculated as the weight loss and ash content was calculated as per ASTM guidelines [24].

Moisture content of the MAC was determined by the sample left after drying. 1 g of the adsorbent was added to 2 mL capacity of the predried and tared capsule. Then the capsule was placed in an oven at 150 °C for 3 h. After cooling in a desiccator to ambient temperature, the weight of the capsule with the material was measured [24].

The sample was predried at 150 °C before making the calculation of apparent density. Dried sample was placed in a 100 mL cylinder up to the 50 mL mark using a funnel. The cylinder was inspected to ensure that the contents were uniformly packed. The content of the cylinder was transferred to a balance pan and weighed [24].

The morphology of the prepared material was analyzed using scanning electron microscope (Hitachi S-4800, EDS PV7747/17 ME).

2.2.2. Chemical characterizations

MAC composition was determined by energy dispersive X-ray analysis. Surface functionalities of the adsorbent were studied using a Fourier transform infrared spectroscope (FTIR 8201 Shimadzu spectrometers). The spectra were recorded within the range of 500–4000 cm^{-1}. Significant surface functional groups have been determined by comparing the recorded bands with standard frequency patterns. The surface charge of MAC and pH_{zpc} were determined using a Malvern Zetasizer at different pH values with 0.1 N HCl and 0.1 N NaOH electrolytes.

2.3. Quantification of Ibu

A numbers of instruments/methods such as tandem mass spectrometry (LC-MS/MS), gas chromatography–mass spectrometry (GC–MS), HPLC-MS/MS, UV and FTIR spectroscopy were used for the analysis of Ibu present in water. It is generally suggested that NSAID samples be concentrated by a method such as solid-phase

extraction, liquid phase extraction or solid phase micro extraction before their analysis [25–27].

GC-FID has been used for the determination of Ibu concentration in water. The apparatus consisted of an Agilent Technologies GC 6890N system, equipped with a Agilent 7683 series autosampler and a 7683B series injector. The column used was HP-5, Agilent product 1909J-413, with a 5% phenyl methyl siloxane (PMS) capillary of dimensions 30.0 m × 320 μm × 0.25 μm. Helium was used as a carrier gas and the inlet pressure was 6.16 psi, corresponding to a flow rate of 1 mL/min. Injection was made in splitless mode at an injector temperature of 280 °C. The GC programs were set as 80 °C (1 min), 200 °C at a rate of 10 °C min^{-1} (1 min), 260 °C at a rate of 15 °C min^{-1}, and finally 300 °C at a rate of 3 °C min^{-1}.

The analysis of the ibuprofen involves three steps: extraction, derivatization and finally GC-FID analysis. Solid phase extraction (SPE extractions) was performed using a J.T. Baker-Baker SPE 12G Visiprep DL Vacuum Manifold for 12 samples (Prod. No. 7018.94) from Supelco (Bellefonte, PA, USA). SPE was done using Chromabond Octadecyl-modified silica end capped (C-18 ec) cartridges treated with 1.5 mL methanol and 4.5 mL water. Samples (2 mL) were extracted at a rate of 1.5 mL/min. Vacuum dried cartridges were eluted with 0.5 mL methanol in triplicate. The eluants were dried with flowing nitrogen. 0.5 mL of BSTFA was added to the residue and vials were kept in an oven at 60 °C for 30 min.

2.4. Adsorption of Ibu on MAC surfaces

Experiments examining adsorption of Ibu on MAC were conducted by optimizing the varying parameters viz. pH, contact time, temperature and concentration of the adsorbate. The pH value was varied from 2 to 8. Before mixing the MAC in spiked solution, the desired pH for each solution was obtained using 0.1 N HCl and 0.1 N NaOH. All the experiments were carried out in batch mode. 20 mL of 10 mg/L of Ibu was placed in a 100 mL stoppered conical flask and 40 mg of the MAC was added to each flask. The stoppered flasks were kept in an incubator shaker at 200 rpm for constant mixing of MAC and Ibu for 5 h. Then the samples were filtered with 0.45 μm polypropylene filters. Temperature was varied from 25 to 45 °C to evaluate the thermodynamic parameters. Experiments were conducted in triplicate to reduce experimental errors. The concentration of adsorbate retained in the adsorbent phase can be calculated as:

$$q_e = \frac{(C_0 - C_e)}{M_{MAC}} \quad (1)$$

2.5. Equilibrium assays

Equilibrium data were analyzed using the well-known Langmuir, Freundlich and Langmuir–Freundlich isotherm models. Accurately weighed amounts of MAC were stirred in an incubator shaker at 200 rpm with 20 mL of adsorbate sample of concentrations varying from 10 to 50 mg/L at 25 °C. The Ibu solution was kept a constant pH of 2. After equilibration, the contents of the flasks were analyzed to determine the concentration of the remaining Ibu.

The Langmuir model is the most widely used isotherm equation for predicting adsorption data, and it assumes uniform energies for monolayer adsorption [28]. The non-linear equation can be written as:

$$q_e = \frac{(Q_m k_l C_e)}{(1 + K_l C_e)} \quad (2)$$

In the Freundlich model, the expression is an exponential equation and assumes heterogeneous adsorption of the adsorbate on the surface [29]. The non-linear equation can be represented as:

$$q_e = k_f C_e^n f \quad (3)$$

The Langmuir–Freundlich model has been found most suitable for predicting equilibrium data [30]. The non-linear Langmuir–Freundlich isotherm equation can be represented as [30]:

$$q_e = \frac{(Q_m k_{lf} C_e^n)}{(1 + k_{lf} C_e^n)} \quad (4)$$

If the value of n is equal to 1, then this equation will become the Langmuir equation. Alternatively, as either C_e or k_{lf} approaches 0, this isotherm reduces to the Freundlich isotherm.

2.6. Kinetics assays

A number of kinetic models are available to describe adsorption mechanisms but most of them use Ho's pseudo second-order kinetic model [31], which represents experimental kinetic data well for the entire adsorption period for most adsorbate–adsorbent systems. Here we applied the pseudo second-order, pseudo-first order and Elovich model [31–33] to our data. The kinetic data were also analyzed using the intraparticle diffusion model to determine the mechanism of the adsorption process.

The Lagergren and Ho equations were used for pseudo first- and pseudo second-order kinetics can be written as:

$$q_t = q_e - \left(\frac{q_e}{10^{k_1 t/2.303}}\right) \quad (5)$$

$$q_t = \frac{(q_e^2 k_2 t)}{(1 + q_e k_2 t)} \quad (6)$$

The Elovich equation was used to describe sorption behavior with a rapid equilibrium rate in the early period and slower equilibrium rates at later periods of the sorption process [34]. The Elovich equation was applied to chemisorptions and validated the systems in which the adsorbing surfaces were heterogeneous. The rate equation was simplified by Chein and Clayton [35] and can be written as:

$$q_t = \frac{1}{\beta(\ln \alpha\beta)} + \frac{1}{\beta(\ln t)} \quad (7)$$

In the past, many reports have successfully discussed the mechanism of sorption kinetics by considering the intra-particle diffusion model, by plotting adsorbent capacity at time t against square root of time. The intraparticle diffusion equation is as follow:

$$q_t = k_{ipd}\sqrt{t} + C \quad (8)$$

2.7. Thermodynamic analysis

Thermodynamic parameters were evaluated to determine Gibbs free energy, which indicates the spontaneity of the adsorption. A higher negative value of the Gibbs free energy change indicates a more favorable adsorption. It can be represented as:

$$\Delta G^\circ = -RT \ln K \quad (9)$$

The relationship between equilibrium constant and temperature is given by the van't Hoff equation as:

$$\ln K = \frac{-(\Delta H^\circ)}{RT} + \frac{(\Delta S^\circ)}{R} \quad (10)$$

ΔH° and ΔS° can be calculated from the plot of ln K against $1/T$.

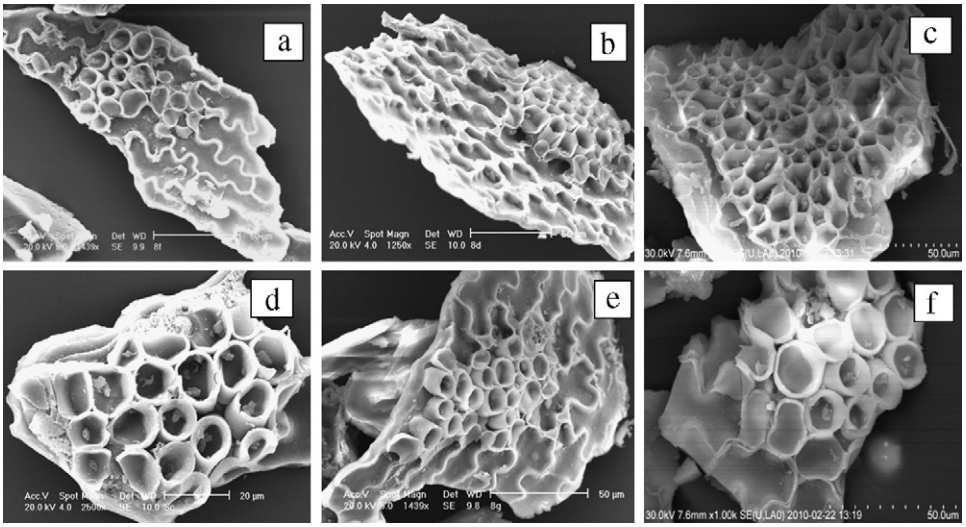

Fig. 1. Scanning electron micrographs of different MAC particles.

2.8. Statistical analysis

In order to estimate the best fit of the kinetic and equilibrium models to the experimental equilibrium and kinetic data, the optimization procedure requires different statistical parameters to be defined. In this study, the best fit model was evaluated by S.D., r^2, F value, and χ^2. The experimental data were analyzed using Microcal Origin (version 8) computer software. If the data from the model are similar to the experimental data, S.D. and χ^2 will be small numbers, r^2 will be around 1 and the F value will be a large number. Therefore it is necessary to analyze the data set using several statistical values to confirm the best-fit kinetics and isotherm for the adsorption system.

3. Results and discussions

3.1. Characterizations

The results of the physical characterization of MAC, i.e. ash content, moisture content, apparent density and pore size, were shown in Table 1. The ash content of activated carbon was the non-combustible residue left after burning of the activated carbon at high temperature. It was reduced the overall activity and efficiency of the activated carbon. The ash content of MAC was 3.36%, which was good for the reactivation of MAC. The moisture content and apparent density of the MAC were 1.17% and 0.66 cc/g, respectively. Elemental composition of the MAC was obtained from the EDX graph and was presented in Table 1.

The porous structures of MAC were revealed under scanning electron microscopy examination, with individual particles were displaying intensely convoluted porosities (honeycomb-structured surface morphology) (Fig. 1a–f). The N_2 gas adsorption/desorption curve was presented in Fig. 2. The surface area and porosity of the MAC calculated from the N_2 adsorption–desorption graph were 358.20 m^2/g and 2.46 nm, respectively, confirming the adequate surface area and good in agreement to mesoporosity of the surface structure.

Fig. 3 shows the pH versus ζ potential (mV) curves for MAC at ionic strengths of 0.1 N HCl and 0.1 N NaOH. The pH_{zpc} value was 5.05, which indicated the MAC surface was positive in nature up to this pH and became negative as the pH increased beyond 5.05. IR spectra allowed surface functionalities to be identified, and relevant peaks were described in Table 2.

Table 1
Mugwort activated carbon: physical and chemical characteristics.

Characterizations	Results
Surface area (m^2/g)	358.20
Pore volume (cc/g)	0.21
Pore size (nm)	2.46, mesoporous material
Ash content (%)	3.36
Moisture content (%)	1.17
Apparent density (g/cm^3)	0.66
ζ-potentiometer	5.05
SEM	Honeycomb like surface morphology
EDX (elemental composition)	C (75.84%), N (0.32%), O (21%), S (0.79%)

3.2. Equilibrium assay

Langmuir, Freundlich and Langmuir–Freundlich models were applied to evaluate the adsorption capacity of MAC for Ibu (Fig. 4). The adsorption capacity was calculated from the best fitted model. All three models were applied to the equilibrium data and the values calculated from the graph were presented in Table 3. The Freundlich model was not well supported by the statistical analysis. In the case of the Langmuir–Freundlich model, r^2 value was

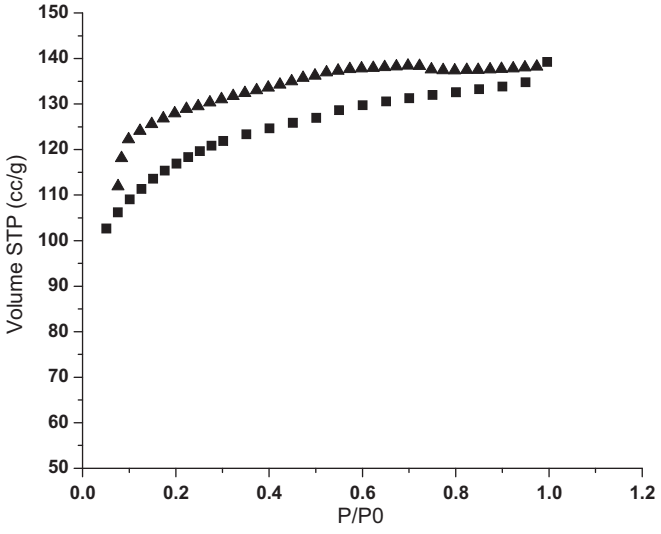

Fig. 2. Adsorption–desorption of N_2 on MAC surface.

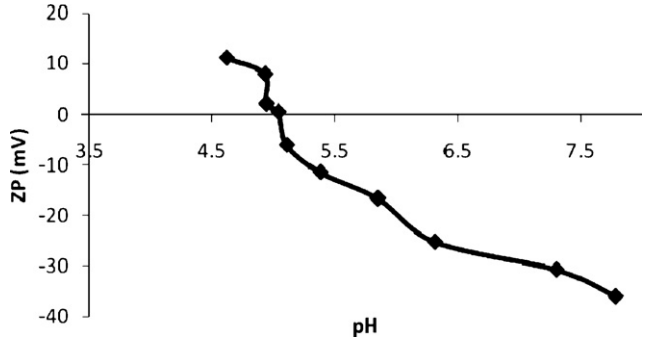

Fig. 3. Variation of ζ potential value with different pH.

Table 2
IR spectra and assigned peaks for different functional groups.

Wave numbers (cm^{-1})	Assigned functional groups
3400–3500 (broad peak)	Hydroxy group, H-bonded OH stretch and amide N–H stretch peak in the same region
2921 and 2851.2	Methyl C–H asym str. and sym str., respectively
3020.0, 1978.1, 1450.9 and 804.9	Aromatic C–H stretching, C=C ring stretch, C=C aromatic ring stretch, C–H bending
1651.9 and 1516.9	Amide C=O stretch and Amide N–H bending
1384.2	C–N stretch
1024.4	C–O stretch

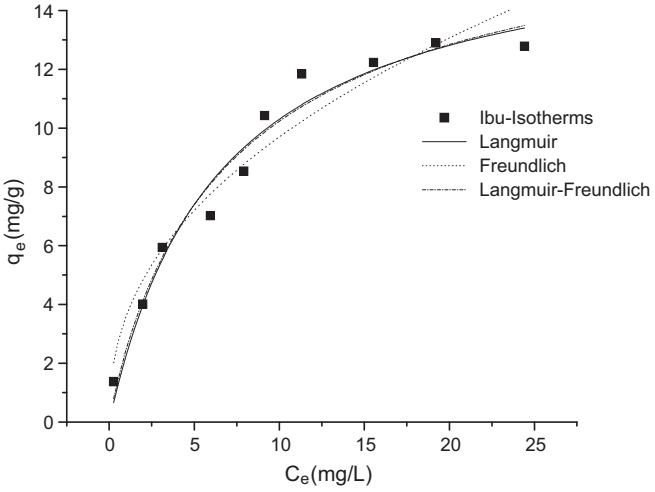

Fig. 4. Isotherm for Ibu adsorption (adsorbate concentration, 10–50 mg/L; contact time, 5 h; agitation speed, 200 rpm; temperature, 25 °C; adsorbent quantity, 40 mg; adsorbate quantity, 20 mL; pH 2).

Table 3
Different isotherm parameters evaluated for Ibu adsorption.

Isotherm	Parameters	Ibu
Langmuir	k_l	0.155
	q_m	16.945
	SD	0.742
	r^2	0.969
	χ^2	0.551
	F value	816.800
Freundlich	k_f	19.693
	n_f	2.325
	SD	0.993
	r^2	0.946
	χ^2	0.986
	F value	454.164
Langmuir–Freundlich	q_m	17.995
	k_{lf}	0.159
	n	0.918
	SD	0.787
	r^2	0.970
	χ^2	0.619
	F value	483.559

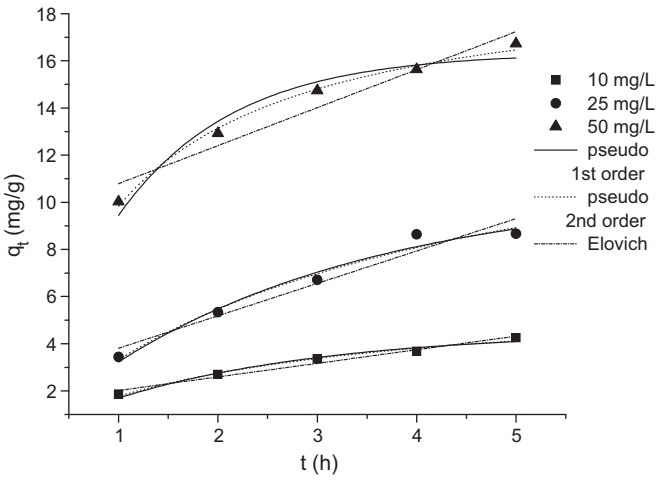

Fig. 5. Different kinetics for Ibu (adsorbate concentration, 10, 25, 50 mg/L; contact time, 5 h; agitation speed, 200 rpm; temperature, 25 °C; adsorbent quantity, 40 mg; adsorbate quantity, 20 mL; pH 2).

(0.970) which was comparable to Langmuir model (r^2 0.969). However, the higher value of F (816.800) and lower values of S.D. (0.742) and χ^2 (0.551) for the Langmuir model made it a better model for Ibu adsorption than Langmuir–Freundlich (F 483.559; S.D. 0.787; χ^2 0.619).

3.3. Kinetics of Ibu adsorption

In this work the kinetics for Ibu adsorption onto MAC were studied at different adsorbate concentrations. By interpreting the kinetic experimental data, the rate-limiting step, which was a significant factor in determining the mechanism of the adsorption process, could be predicted [36].

The plots of pseudo first-order, pseudo second-order and Elovich kinetics were presented in Fig. 5 for Ibu adsorption. Though the experimental q_e value was found to be in good agreement with the calculated q_e value for the pseudo first-order equation, it had lower r^2 and F values than the other kinetic models (Table 4). Also, the S.D. and χ^2 values were higher than those for the pseudo second-order and Elovich models. The statistical parameters for pseudo first-order models obtained for Ibu adsorption were low. Therefore, the adsorption system described here did not of pseudo first-order kinetics. On the other hand, the pseudo second-order model showed a satisfactory correlation coefficient and other statistical values when compared to the experimental data related to Ibu adsorption onto MAC. Elovich constants α and β were calculated from the intercept and the slopes of the lines for Ibu adsorption on MAC and were presented in Table 4 with all the statistical values. It could be seen that with the increase in concentration of adsorbate, the constant α increased, indicating that Ibu absorption increased, but the constant β decreased at constant adsorbent quantity. Pseudo second-order was found the most fitted model for Ibu adsorption, among all the tested kinetic models, with good correlation values: r^2 (0.987–0.993), F (1745.420–8300.450), S.D. (0.124–0.247) and χ^2 (0.015–0.061).

In the case of solid–liquid adsorption processes, the adsorbate transfer to the adsorbent surface was interpreted as either external mass transfer for non-porous surfaces or intra-particle diffusion for porous surfaces, or both. Although the intra-particle diffusion model did not provide a reaction rate, it had been correlated with system variables to characterize the influence of intra-particle diffusion in adsorption mechanisms. It could be seen that intra-particle diffusion was the major rate-determining step in the adsorption process (Table 4). The value of k_{ipd} was var-

Table 4
Different rate order parameters evaluated for Ibu adsorption.

Kinetic model	Parameters	Ibu		
		10 mg/L	25 mg/L	50 mg/L
Pseudo 1st order	q_e (equation)	4.255	8.665	16.730
	q_e (plot)	4.530	10.588	16.340
	k_1	0.469	0.364	0.863
	SD	0.169	0.402	0.614
	r^2	0.975	0.976	0.959
	χ^2	0.029	0.162	0.377
	F value	930.24	724.64	1337.26
Pseudo IInd order	q_e (equation)	4.255	8.665	16.730
	q_e (plot)	6.195	15.453	19.800
	k_2	0.064	0.018	0.049
	SD	0.124	0.403	0.247
	r^2	0.987	0.976	0.993
	χ^2	0.015	0.162	0.061
	F value	1745.420	723.120	8300.450
Elovich	α	7.014	8.068	479.225
	β	1.735	0.727	0.621
	SD	0.159	0.604	0.741
	r^2	0.977	0.945	0.940
	χ^2	0.026	0.365	0.549
	F value	1047.920	320.476	916.486
Intraparticle diffusion	k_{ipd}	1.889	4.528	5.349
	C	0.003	−1.033	5.044
	SD	0.079	0.439	0.413
	r^2	0.995	0.971	0.982
	χ^2	0.006	0.193	0.171
	F value	4332.880	608.590	2957.680

ied from 1.889 to 5.349 mg/g h for Ibu adsorption, for adsorbate concentrations ranging from 10 to 50 mg/L, respectively. All the statistical parameters for Ibu adsorption, r^2 (0.995–0.982), F value (4332.880–2957.680), S.D. (0.079–0.413) and χ^2 (0.006–0.171), supported the applicability of the intra-particle diffusion model.

3.4. Thermodynamic parameters at equilibrium

The thermodynamic parameters were appropriately evaluated to obtain information regarding free energy change, enthalpy change and entropy change for the adsorption. The thermodynamic parameters ΔG°, ΔH° and ΔS° were obtained from the $\ln K_c$ versus $1/T$ plot. The plots showed good correlation coefficient values for Ibu (r^2 0.982). The value of K_c for Ibu were varied from 2.025 to 8.759 in temperature range of 298–318 K. The corresponding ΔG° values from temperature 298 to 318 °C were (−1.745) to (−5.728) kJ/mol. The ΔH° and ΔS° were (+57.455) kJ/mol and (+198.166) J/mol K, respectively (Table 5). A positive value of ΔH° for Ibu removal from MAC surfaces indicated the endothermic nature of the process, and the negative value of the free energy indicated the spontaneous nature of the adsorption process. It was also noticed that the change in free energy increased with temperature, which showed that adsorption was improved with rising temperature. This could be due to activation of more sites on the MAC surface at higher temperature.

3.5. Effect of pH on Ibu adsorption

The pH of the reaction solution played an important role in the adsorption process by influencing the surface properties of the adsorbent. As evident from the chemical characterization of MAC, pH_{zpc} of the surface was about 5.05. Experiments were carried out at different pH values from 2 to 8 (Fig. 6). The surface charge of the MAC was varied with pH from positive to negative at pH values lower and higher than the pH_{zpc} value, respectively.

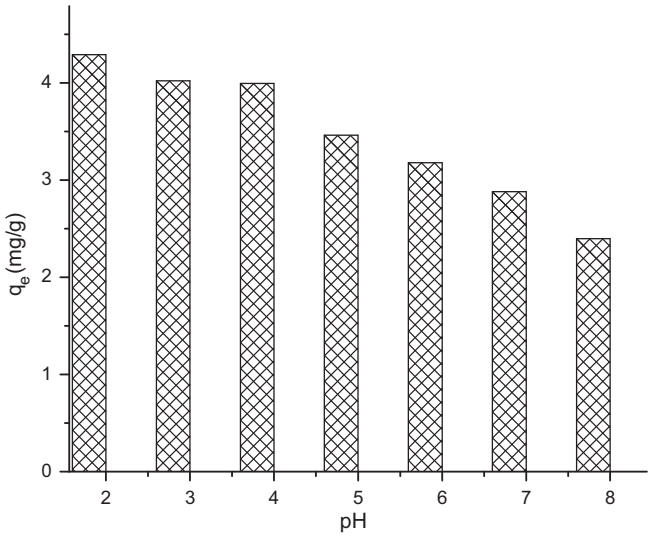

Fig. 6. Adsorption of Ibu at different pH (adsorbate concentration, 10 mg/L; contact time, 5 h; agitation speed, 200 rpm; temperature, 25 °C; adsorbent quantity, 40 mg; adsorbate quantity, 20 mL).

At the acidic pH, there was dissociation of molecule into the proton and carboxylate anion. As the pH_{zpc} of the MAC was 5.05,

Table 5
Free energy change, enthalpy change and entropy change for Ibu adsorption (R: 8.300 × 10^{-3} kJ/mol K).

	T (K)	K_c	ΔG (kJ/mol)	ΔH (kJ/mol)	ΔS (J/mol K)	r^2
Ibu	298	2.025	−1.745			
	308	3.632	−3.297	57.455	198.166	0.982
	318	8.759	−5.728			

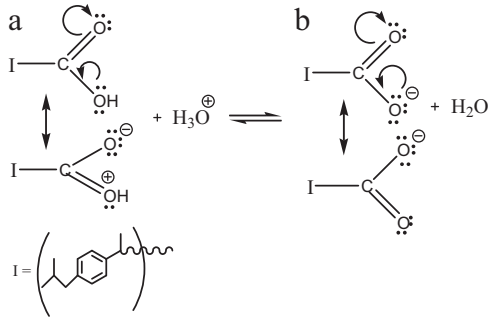

Fig. 7. Stabilized resonating structure of Ibu molecule (a) by charge separation (b) by charge delocalization.

above this pH the surface of the activated carbon had more negative charge and hindered the adsorption of the negatively charged ibuprofen. Hence more adsorption was observed at lower pH, and the maximum adsorption was found to occur in the range of pH 2–4. A tentative mechanism was presented below (Figs. 7 and 8).

3.6. Mechanistic evaluation

The biologically-derived activated carbon described here was analyzed in terms of its surface area, porosity, different chemical functionalities, overall surface charge, and morphological profile to understand the probable mechanism of Ibu removal from water. The MAC characteristics were summarized in Table 1.

Fig. 7 showed the Ibu molecule is itself resonance stabilized in aqueous medium as the molecule has a carboxyl functional group. Either a small amount of resonance stabilization is achieved by charge separation, as in Fig. 7a, or a large amount of resonance stabilization is achieved by charge delocalization, as in Fig. 7b. Overall, the adsorbent surface was positively charged at lower pH, as indicated by the ζ potentiometer result. These findings were resulted for electrostatic attraction between the negatively charged sorbate (Ibu) and positively charged sorbent (MAC); thus, Ibu molecules adhered to the MAC surfaces.

Hydroxyl, amide region, benzene and alkyl region peaks were identified from FTIR spectroscopy and were in good agreement with the EDX data for C, O, H and N. These various functionalities also took part in the chemisorption of Ibu molecules. One of the probable mechanisms could be the interaction between the methyl substituted amide (–$CONHCH_3$) functional group of MAC and resonance stabilized adsorbate; that could formed a six-membered stable ring as a result of dipolar interactions, as in Fig. 8. Cuts and grooves along with cavities similar to mass wax cells of honeycomb were observed by SEM micrograph on the surfaces of MAC, signifying its porous nature. The porosity of the activated carbon would also assisted Ibu

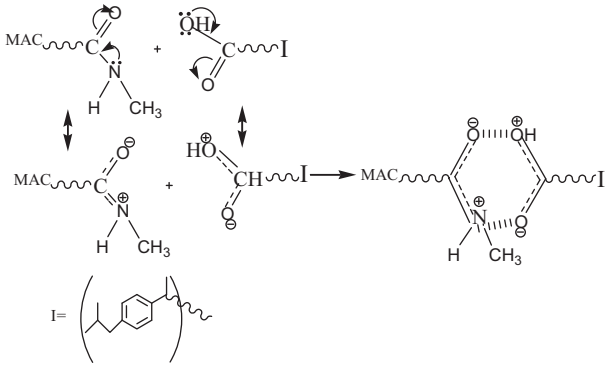

Fig. 8. Adsorption of Ibu by MAC surface.

adsorption. The Ibu molecule could be trapped within mesoporous material having a pore size of 2.46 nm. The MAC surface area was 358.20 m^2/g, as measured with a BET surface area analyzer, which would provide a larger surface area for adsorbate.

4. Conclusions

We were successful in synthesizing the mesoporous activated carbon from the leaves of the invasive weed, mugwort, which could be an improved adsorbent for Ibu. Maximal adsorption of Ibu by MAC was at pH 2. Pseudo second-order kinetics was the most accurate for Ibu adsorption, with intra-particle diffusion successfully predicted the mechanism of adsorption kinetics. The results showed that the adsorption equilibrium data were fitted best using a Langmuir model in the studied concentration range for Ibu adsorption. The negative value of ΔG° confirmed/substantiated Ibu adsorption on MAC surfaces and the positive value for ΔH° indicated the endothermic nature of the process. Conclusively, the synthesized activated carbon from mugwort leaves may be a suitable adsorbent for the removal of Ibu. It may also be useful for other catalytic purposes.

Acknowledgments

The authors are pleased to acknowledge the European Commission (Brussels) for the Marie Curie Research Fellowship for Transfer of Knowledge (No. MTKD-CT-2006-042637) and Council of Science & Technology, Lucknow, India for financial supports. The authors are grateful to Eveliina Repo (M.Sc.), for her assistance in surface area analysis.

References

[1] M.A. Shannon, P.W. Bohn, M. Elimelech, J.G. Georgiadis, B.J. Marinas, A.M. Mayes, Science and technology for water purification in the coming decades, Nature 452 (2008) 301–310.
[2] M. Sillanpää, M. Orama, J. Rämö, A. Oikari, The importance of ligand speciation in environmental research: a case study, Sci. Total Environ. 267 (2001) 23–31.
[3] S.L. Percival, J.T. Walker, P.R. Hunter, Microbiological Aspects of Biofilms and Drinking Water, CRC Press, Boca Raton, FL, 2000.
[4] B. Halling-Sørensen, S.N. Nielsen, P.F. Lanzky, F. Ingerslev, H.C. Holten Lützføft, S.E. Jørgensen, Occurrence, fate and effects of pharmaceutical substances in the environment–a review, Chemosphere 36 (1998) 357–393.
[5] S. Weigel, J. Kuhlmann, H. Hühnerfuss, Drugs and personal care products as ubiquitous pollutants: occurrence and distribution of clofibric acid, caffeine and DEET in the North Sea, Sci. Total Environ. 295 (2002) 131–141.
[6] S.K. Khetan, T.J. Collins, Human pharmaceuticals in the aquatic environment: a challenge to green chemistry, Chem. Rev. 107 (2007) 2319–2364.
[7] C. Nebot, S.W. Gibb, K.G. Boyd, Quantification of human pharmaceuticals in water samples by high performance liquid chromatography–tandem mass spectrometry, Anal. Chim. Acta 598 (2007) 87–94.
[8] T.A. Ternes, Occurrence of drugs in german sewage treatment plants and rivers, Water Res. 32 (1998) 3245–3260.
[9] M. Farré, I. Ferrer, A. Ginebreda, M. Figueras, L. Olivella, L. Tirapu, M. Vilanova, D. Barceló, Determination of drugs in surface water and wastewater samples by liquid chromatography–mass spectrometry: methods and preliminary results including toxicity studies with *Vibrio fischeri*, J. Chromatogr. A 938 (2001) 187–197.
[10] S. Öllers, H.P. Singer, P. Fässler, S.R. Müller, Simultaneous quantification of neutral and acidic pharmaceuticals and pesticides at the low-ng/l level in surface and waste water, J. Chromatogr. A 911 (2001) 225.
[11] R. Andreozzi, M. Raffaele, P. Nicklas, Pharmaceuticals in STP effluents and their solar photodegradation in aquatic environment, Chemosphere 50 (2003) 1319–1330.
[12] P. Westerhoff, Y. Yoon, S. Snyder, E. Wert, Fate of endocrine-disruptor, pharmaceutical, and personal care product chemicals during simulated drinking water treatment processes, Environ. Sci. Technol. 39 (2005) 6649–6663.
[13] S.S. Mahmoud, M.A. Hassan, F.H. El-Khatib, A.A. Obaidat, M. Sheikh-Salem, The kinetics of tenoxicam photodegradation in solution, React. Kinet. Catal. Lett. 70 (2000) 119–124.
[14] F. Mendez-Arriagad, R.A. Torres-Palmaa, C. Petriera, S. Esplugasd, J. Gimenezd, C. Pulgarin, Ultrasonic treatment of water contaminated with ibuprofen, Water Res. 42 (2008) 4243–4248.
[15] L. Ciríaco, C. Anjo, J. Correia, M.J. Pacheco, A. Lopes, Electrochemical degradation of Ibuprofen on Ti/Pt/PbO_2 and Si/BDD electrodes, Electrochim. Acta 54 (2009) 1464–1472.

[16] A.V. Dordioa, A.J. Estêvão Candeiasa, A.P. Pintoa, C. Teixeira da Costaa, A.J. Palace Carvalho, Preliminary media screening for application in the removal of clofibric acid, carbamazepine and ibuprofen by SSF-constructed wetlands, Ecol. Eng. 35 (2009) 290–302.
[17] A. Rossner, S.A. Snyder, D.R.U. Knappe, Removal of emerging contaminants of concern by alternative adsorbents, Water Res. 43 (2009) 3787–3796.
[18] A. Dordio, A.J. Palace Carvalho, D.M. Teixeira, C.B. Dias, A.P. Pinto, Removal of pharmaceuticals in microcosm constructed wetlands using *Typha* spp. and LECA, Bioresour. Technol. 101 (2010) 886–892.
[19] A.S. Mestre, J. Pires, J.M.F. Nogueira, J.B. Parra, A.P. Carvalho, C.O. Ania, Waste-derived activated carbons for removal of ibuprofen from solution: role of surface chemistry and pore structure, Bioresour. Technol. 100 (2009) 1720–1726.
[20] T.X. Bui, H. Choi, Adsorptive removal of selected pharmaceuticals by mesoporous silica SBA-15, J. Hazard. Mater. 168 (2009) 602–608.
[21] A.S. Mestre, J. Pires, J.M.F. Nogueira, A.P. Carvalho, Activated carbons for the adsorption of ibuprofen, Carbon 45 (2007) 1979–1988.
[22] K.G. Ramawat (Ed.), Biotechnology of Medicinal Plants: Vitalizer and Therapeutic, vol. 5, Enfield, New Hampshire, Science Publishers Inc., 2004.
[23] M. Himly, B. Jahn-Schmid, A. Dedic, P. Kelemen, N. Wopfner, F. Altmann, R.V. Ree, P. Briza, K. Richter, C. Ebner, F. Ferreira, The major allergen of mugwort pollen, is a modular glycoprotein with a defensin-like and a hydroxyproline-rich domain, FASEB J. 17 (2003) 106–108.
[24] ASTM, Refractories; Carbon and Graphite Products; Activated Carbon. Annual Book of ASTM Standards, vol. 15.01, 1995.
[25] I. González-Mariño, J.B. Quintana, I. Rodríguez, R. Cela, Determination of drugs of abuse in water by solid-phase extraction, derivatization and gas chromatography–ion trap-tandem mass spectrometry, J. Chromatogr. A 1217 (2010) 1748–1760.
[26] T. Einsle, H. Paschke, K. Bruns, S. Schrader, P. Popp, M. Moeder, Membrane-assisted liquid–liquid extraction coupled with gas chromatography–mass spectrometry for determination of selected polycyclic musk compounds and drugs in water samples, J. Chromatogr. A 1124 (2006) 196–204.
[27] H. Lord, J. Pawliszyn, Microextraction of drugs, J. Chromatogr. A 902 (2000) 17–63.
[28] I. Langmuir, The adsorption of gases on plane surfaces of glass, mica and platinum, J. Am. Chem. Soc. 40 (1918) 1361–1367.
[29] H.M.F. Freundlich, Over the adsorption in solution, J. Phys. Chem. 57 (1906) 385–470.
[30] R.J. Umpleby II, S.C. Baxter, Y. Chen, R.N. Shah, K.D. Shimizu, Characterization of Molecularly Imprinted Polymers with the Langmuir–Freundlich Isotherm, Anal. Chem. 73 (2001) 4584.
[31] Y.S. Ho, G. McKay, D.A.J. Wase, C.F. Foster, Study of the sorption of divalent metal ions on to peat, Adsorp. Sci. Technol. 18 (2000) 639–650.
[32] S. Lagergren, About the theory of so-called adsorption of soluble substances, Kungliga Svenska Vetenskapsakademiens Handlingar 24 (1898) 1–39.
[33] S.J. Elovich, in: J.H. Schulman (Ed.), Proceedings of the Second International Congress on Surface Activity, vol. 11, Academic Press Inc., New York, 1959, p. 253.
[34] C.-F. Chang, C.-Y. Chang, K.-H. Chen, W.-T. Tsai, J.-L. Shie, Y.-H. Chen, Adsorption of naphthalene on zeolite from aqueous solution, J. Colloid Interface Sci. 277 (2004) 29–34.
[35] S.H. Chein, W.R. Clayton, Application of Elovich equation to the kinetics of phosphate release and sorption in soil, J. Am. Soil Sci. Soc. 44 (1980) 265–268.
[36] V. Vadivelan, V.K. Kumar, Equilibrium, kinetics, mechanism, and process design for the sorption of methylene blue onto rice husk, J. Colloid Interface Sci. 286 (2005) 90–100.